JOURNAL OF MAGNETIC RESONANCE **125,** 245–258 (1997)
ARTICLE NO. MN971111

Time-Reverse ODESSA. A 1D Exchange Experiment for Rotating Solids with Several Groups of Equivalent Nuclei

D. REICHERT,* H. ZIMMERMANN,† P. TEKELY,‡ R. POUPKO§ AND Z. LUZ§

*Martin-Luther Universität Halle-Wittenberg, Fachbereich Physik, 06108 Halle, Germany; †Max-Planck-Institut für Medizinische Forschung, AG Molekülkristalle, 69028 Heidelberg, Germany; ‡Laboratoire de Méthodologie RMN, URA CNRS, 406 Université H. Poincaré, Nancy 1, France; §Weizmann Institute of Science, 76100 Rehovot, Israel

Received September 3, 1996

A one-dimensional exchange experiment is proposed for magic-angle-spinning samples with several groups of equivalent nuclei undergoing internal exchange, such as pure reorientation, as opposed to mutual exchange. The method, which we term time-reverse ODESSA, is an extension of the recently proposed 1D ODESSA experiment for a single group of exchanging nuclei. When several different groups of spins are present, as is usually the case for carbon-13 in polymers and molecular crystals, the normal ODESSA spectrum yields phase-twisted spectra which are difficult to analyze quantitatively. This problem is solved in the time-reverse ODESSA experiment which yields pure absorption spectra for all families of side bands, as long as only internal exchange need be considered. The experiment consists of the usual three pulse sequence of 2D exchange, $P1—t_1—P2—\tau_m—P3—t_2$ (acquisition), except that the evolution time is fixed at half a rotation period, $t_1 = T_R/2$, the mixing time is set to an odd number of half rotation periods, $\tau_m = (2G - 1)T_R/2$, and the acquisition starts at $t_2 = T_R/2$ after the detection pulse, $P3$. The method is demonstrated using the carbon-13 spectra of dimethyl sulfone and an enriched sample of tropolone, and is applied to the study of the π flip of the inner benzene ring of 1,4-diphenoxybenzene. The scope and limitations of the method are discussed.

INTRODUCTION

Chemical or spin exchange between different types of carbon-13 (or other) nuclei in the solid state, in the slow-exchange regime, where $1/T_2 > k \geqslant 1/T_1$, can be studied under magic-angle spinning (MAS) by various polarization-transfer experiments (*1–3*). For example, the approach to equilibrium can be monitored after selectively inverting the magnetization of one component in a spin multiplet. The extension to pure reorientation, or internal spin exchange within the same group of equivalent nuclei, is more complicated since it involves polarization transfer between different spinning side bands belonging to the same chemical species. The most direct way to do this is by the rotor-synchronized 2D exchange method, first proposed by Veeman and coworkers (*4*) and later modified by Hagemeyer *et al.* (*5*). In this experiment, the mixing time is synchronized with the rotor period, and the resulting cross peaks provide quantitative information on dynamic processes even if only equivalent nuclei are involved (*6–8*).

Such two-dimensional experiments are often very time consuming, and it is therefore desirable to use, whenever possible, equivalent 1D methods. In these 1D experiments, the spin system is prepared in a nonequilibrium state that is modified during the following mixing time by some dynamic process. The first such 1D exchange experiment for equivalent nuclei in rotating solids was designed by Yang *et al.* (*9*). It consists of a preparation period during which the spinning side bands are suppressed by a TOSS sequence, a variable mixing period τ_m, during which spin exchange will mismatch the TOSS conditions, followed by a detection period in which the restoration of the spinning side bands is monitored. The experiment is, however, very sensitive to the exact setting of the TOSS conditions.

An alternative MAS 1D exchange experiment, suitable for monitoring spin exchange between equivalent nuclei, was recently proposed by Gérardy-Montouillout *et al.* (*10*). The experiment was termed ODESSA for *o*ne-*d*imensional *e*xchange *s*pectroscopy by *s*ideband-*a*lternation. It consists of the usual three-pulse sequence of 2D exchange spectroscopy, $P1—t_1—P2—\tau_m—P3—t_2$(acquisition), but with the preparation time fixed at half a rotation period, $t_1 = T_R/2$, and the mixing time set to an integral number of rotation periods, $\tau_m = GT_R$, as shown in Fig. 1a. Under these experimental conditions, the initial magnetic polarization at $\tau_m = 0$ associated with odd spinning side bands is reversed with respect to the even ones. Dynamic processes during the mixing time redistribute the polarization between the various spinning side bands, resulting in a modified MAS spectrum. Analysis of such spectra as a function of the mixing time provides information about the mechanism and kinetic parameters of the dynamic processes. The ODESSA experiment works well if the sample consists of a single set of chemically equivalent spins having the same isotropic chemical shift. However, for a system consisting of several inequivalent nuclei with different isotropic chemical shifts, the above procedure results in phase-twisted signals. This

1090-7807/97 $25.00

renders accurate peak intensity measurements quite difficult and limits the scope of the ODESSA experiment to only very simple cases. Dynamic measurements using, for example, carbon-13 in polymers or molecular crystals exhibiting a multitude of peaks are difficult to perform by this method.

In the present work, we show how the normal ODESSA experiment can be extended to systems consisting of several different groups of spins. If one or several of these groups undergo reorientation, this new procedure results in pure-absorption spectra for all families of spinning side bands. However, if the process involves mutual exchange between different groups, it still results in phase distortion. Such situations are better dealt with by the classical magnetization-transfer methods (*1–3*). The procedure we adopt to overcome the phasing problem is similar to that used by Hagemeyer *et al.* (*5*) to produce pure-absorption 2D exchange spectra, where a time-reverse sequence in the t_1 domain is employed.

In the next section, we first describe the phasing problem of the normal ODESSA experiment for a multisignal spectrum and then show how the modified time-reverse experiment can be used to cure the problem. If only pure reorientation processes are involved, the analysis of the spectra follows the same procedure as for the normal ODESSA experiment. For completeness, we also derive expressions for simulating phase-twisted time-reverse ODESSA spectra for the situation where exchange between different types of spins also takes place. Their practical application is, however, limited. In the following section, we present carbon-13 results for both normal and time-reverse ODESSA experiments on dynamic solid-state systems, including the π flips of dimethyl sulfone (*11, 12*), self diffusion in tropolone (*2, 6, 8, 13*), and benzene π flips in 1,4-diphenoxybenzene (*14*).

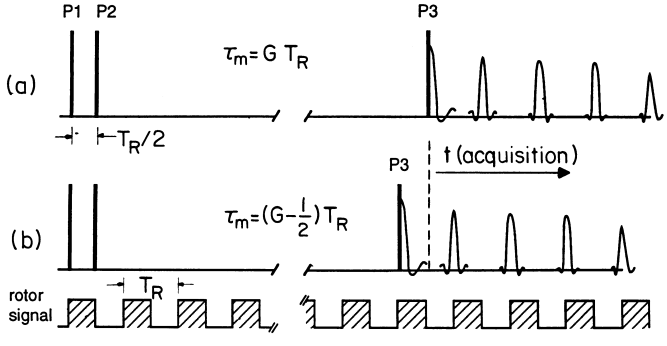

FIG. 1. The normal (a) and the time-reverse (b) ODESSA sequences. *P*1, *P*2, and *P*3 are $\pi/2$ pulses (for carbon-13, *P*1 can also be cross polarization). The preparation time is fixed at half a rotation period, $t_1 = T_R/2$. The mixing time in (a) is an integral number of rotation periods, $\tau_m = GT_R$, and acquisition starts either immediately after *P*3 or T_R later. In (b), the mixing time is an odd-integer number of half rotation periods, $\tau_m = (2G - 1)T_R/2$, and acquisition starts at $T_R/2$ after *P*3. The experiments are initiated by an optical signal reflected from the rotor. A second optical signal, following an approximately set mixing time, initializes a delay, equal to the *P*1 pulse width or the cross-polarization contact time plus $T_R/2$ for the normal experiment, or just the length of *P*1 for the time-reverse experiment, followed by the *P*3 detection pulse. This procedure ensures that the mixing times are GT_R and $(2G - 1)T_R/2$ for the normal and time-reverse experiments, respectively.

TABLE 1
The Four Basic Phase-Cycle Sequences for the Normal and Time-Reverse ODESSA Experiments[a]

	P1	P2	P3	Receiver
1	Y	$-Y$	Y	X
2	$-Y$	$-Y$	Y	$-X$
3	Y	X	Y	$\mp Y$
4	$-Y$	X	Y	$\pm Y$

[a] The upper and lower signs for the receiver phase in sequences 3 and 4 correspond, respectively, to the normal anti-echo and time-reverse echo experiments.

THEORY

A. *Reorientation of a Single Type of Equivalent Nuclei—The Normal ODESSA Experiment*

The pulse sequence for the normal ODESSA experiment (*10*) is shown in Fig. 1a. The basic phase cycle of this experiment consists of four pulse sequences as shown in Table 1. Sequences 1 and 2 yield the phase alternate cosine (Re) component of the evolution period, while sequences 3 plus 4 yield the corresponding sine (Im) component. For a particular crystallite in the sample, characterized by the Euler angles α, β, and γ, with respect to the rotor frame (where γ is the phase angle with respect to the rotor axis), the contribution to the time-domain signal is (*5–7*)

$$ {}^{\mathrm{Re}}_{\mathrm{Im}}G(t;\tau_m) = \sum_{ij} P_{ij}(\tau_m)\,{}^{\mathrm{Re}}_{\mathrm{Im}}G_{ij}(t), \qquad [1] $$

where $P_{ij}(\tau_m)$ is the fractional population of those nuclei which at the beginning of the mixing time were in site j and at its end in site i. These terms are related to the exchange matrix $\mathbf{K}$, by

$$ P_{ij}(\tau_m) = [\exp(\mathbf{K}\tau_m)]_{ij} P_j, \qquad [2] $$

where P_j is the equilibrium population of site j. The ${}^{\mathrm{Re}}_{\mathrm{Im}}G_{ij}(t)$ in Eq. [1] are given by

$$ \begin{aligned} {}^{\mathrm{Re}}_{\mathrm{Im}}G_{ij}(t) = {}&{}^{\mathrm{Re}}_{\mathrm{Im}}\{\exp(i\omega^j_{\mathrm{iso}}T_R/2)\exp[i\theta^j(0, T_R/2)]\} \\ &\times \exp[i\theta^i(T_R/2 + \tau_m, T_R/2 + \tau_m + t)] \\ &\times \exp(i\omega^i_{\mathrm{iso}}t), \end{aligned} \qquad [3] $$

where

$$\theta^k(a, b) = \omega_0 \int_a^b \sigma^k_{\mathrm{an}}(t)dt \qquad [4]$$

$\omega^k_{\mathrm{iso}} = \omega_0\sigma^k_{\mathrm{iso}}$, and σ^k_{iso} and $\sigma^k_{\mathrm{an}}(t)$ are, respectively, the isotropic and time-modulated (by the sample spinning) anisotropic chemical shifts of the nuclei in site k. Similar equations can be written for other anisotropic interactions, such as, for example, the quadrupolar coupling in deuterium MAS NMR (*15*). Using the *f*-function formalism, as described in detail in Refs. (*5, 7, 15*), and recalling that $\omega_R\tau_m = 2\pi G$, Eq. [3] becomes

$$\begin{aligned}{}^{\mathrm{Re}}_{\mathrm{Im}}G_{ij}(t) = {}&{}^{\mathrm{Re}}_{\mathrm{Im}}[\exp(i\omega^j_{\mathrm{iso}}T_R/2)f^j{}^*(\gamma)f^j(\gamma + \pi)] \\ &\times f^i{}^*(\gamma + \pi)f^i(\gamma + \pi + \omega_R t)\exp(i\omega^i_{\mathrm{iso}}t).\end{aligned} \qquad [5]$$

In the normal ODESSA experiment, only a single set of equivalent spins is considered, so that $\omega^j_{\mathrm{iso}} = \omega^i_{\mathrm{iso}} \equiv \omega^a_{\mathrm{iso}}$, and the anisotropic chemical shifts, $\sigma^j_{\mathrm{an}} \equiv \sigma^{aj}_{\mathrm{an}}$ and $\sigma^i_{\mathrm{an}} \equiv \sigma^{ai}_{\mathrm{an}}$, refer to different symmetry-related sites, aj, ai, of the same group of nuclei, a, which are interchanged by the dynamic process. The phase cycle in Table 1 ensures that the anti-echo signal is added in the receiver, so that

$$\begin{aligned}G^+_{ai\,aj} &= {}^{\mathrm{Re}}G_{ai\,aj}(t) + i^{\mathrm{Im}}G_{ai\,aj}(t) \\ &= f^{aj}{}^*(\gamma)f^{aj}(\gamma + \pi)f^{ai}{}^*(\gamma + \pi) \\ &\quad \times f^{ai}(\gamma + \pi + \omega_R t)\exp[i\omega^a_{\mathrm{iso}}(t + T_R/2)].\end{aligned} \qquad [6]$$

Integration over α, β, γ finally yields the overall 1D anti-echo ODESSA signal

$$\begin{aligned}S^+(t; \tau_m) = {}&\exp(i\omega^a_{\mathrm{iso}}T_R/2)\sum_N I^a_N(\tau_m) \\ &\times \exp[i(\omega^a_{\mathrm{iso}} + N\omega_R)t],\end{aligned} \qquad [7]$$

where the coefficients $I^a_N(\tau_m)$ correspond to the side-band intensities

$$I^a_N(\tau_m) = \sum_{ai\,aj} P_{aiaj}(\tau_m)\exp(-\tau_m/T^a_1)I^{ai\,aj}_N \qquad [8]$$

with

$$I^{ai\,aj}_N = \sum_M (-)^M I^{ai\,aj}_{MN} \qquad [9]$$

and where the effect of T_1 during the mixing time has been added. The terms $I^{ai\,aj}_{MN}$ correspond to the cross peaks (or if $i = j$, $M = N$, to diagonal peaks) in the rotor-synchronized 2D exchange experiment (*5*). Their definitions, in terms of the chemical-shift tensors in sites ai and aj and the spinning frequency ω_R, are given in the references cited above. In practice, in the normal ODESSA experiment the carrier frequency is set at the center band frequency so that ω^a_{iso} vanishes, or a constant phase correction ($-\omega^a_{\mathrm{iso}}T_R/2$) is applied, yielding pure-absorption peaks for all spinning side bands.

B. Reorientation of Several Different Groups of Nuclei—The Time-Reverse ODESSA Experiment

We next consider the case where the spin system consists of several distinct groups of equivalent nuclei with different isotropic chemical shifts ω^a_{iso}, $\omega^b_{\mathrm{iso}}, \cdots$ and different anisotropic chemical-shift tensors, $\sigma^{ai}_{\mathrm{an}}$, $\sigma^{aj}_{\mathrm{an}}, \cdots$ $\sigma^{bi}_{\mathrm{an}}$, $\sigma^{bj}_{\mathrm{an}}$, $\cdots$. If we limit ourselves to pure reorientation, summation of Eq. [5] over the various groups yields

$$\begin{aligned}{}^{\mathrm{Re}}_{\mathrm{Im}}G(t; \tau_m) = {}&\sum_a \sum_{ai\,aj} P_{ai\,aj}(\tau_m){}^{\mathrm{Re}}_{\mathrm{Im}}[\exp(i\omega^a_{\mathrm{iso}}T_R/2) \\ &\times f^{aj}{}^*(\gamma)f^{aj}(\gamma + \pi)] \\ &\times f^{ai}{}^*(\gamma + \pi)f^{ai}(\gamma + \pi + \omega_R t) \\ &\times \exp(i\omega^a_{\mathrm{iso}}t).\end{aligned} \qquad [10]$$

Proceeding as above, the anti-echo signal becomes

$$\begin{aligned}S^+(t; \tau_m) = {}&\sum_a \exp(i\omega^a_{\mathrm{iso}}T_R/2)\sum_N I^a_N(\tau_m) \\ &\times \exp[i(\omega^a_{\mathrm{iso}} + N\omega_R)t].\end{aligned} \qquad [11]$$

The spectrum resulting from this signal is phase distorted, because different spinning side-band families are associated with different phase factors, $\omega^a_{\mathrm{iso}}T_R/2$. If we correct the phase of one family of side bands, that of the others is still distorted. Such distortions hamper the intensity measurements even of the pure-absorption peaks in the spectrum, because of the long ''tails'' of nearby unphased peaks. In the following, we propose a modification of the ODESSA experiment that overcomes this problem by canceling the distortion effect of the $\omega^a_{\mathrm{iso}}T_R/2$'s.

The modification involves three elements as shown in Fig. 1b. First, we introduce a $T_R/2$ delay in the acquisition following the *P*3 pulse. This alone will, however, increase the distortion by adding another $\omega^a_{\mathrm{iso}}T_R/2$ twist to the phase of each family of side bands. To make the two phase distortions cancel, we take the echo signal, $G^-(t) = {}^{\mathrm{Re}}G(t) - i^{\mathrm{Im}}G(t)$ of Eq. [10], so that the initial phase becomes $-\omega^a_{\mathrm{iso}}T_R/2$, canceling the $+\omega^a_{\mathrm{iso}}T_R/2$ of the delayed acquisition. This, however, results in complex conjugation of the $f^{aj}{}^*(\gamma)f^{aj}(\gamma + \pi)$ products which causes even more severe intensity and phase distortions. Finally, to correct for this effect, we use the time-reverse method, originally proposed by Hagemeyer *et al.* (*5*) to obtain pure-absorption line shapes in rotor-synchronized 2D exchange spectra. We do so by subtracting half a rotation period from the mixing time

so that it becomes an odd half integral number of rotation periods,

$$\tau_m = (2G - 1)T_R/2 = (G - \tfrac{1}{2})T_R. \quad [12]$$

When these changes are introduced, we obtain for $G(t;\tau_m)$

$$\begin{aligned}{}^{\mathrm{Re}}_{\mathrm{Im}}G(t;\tau_m) = \sum_a \sum_{ai\,aj} P_{ai\,aj}(\tau_m)\,{}^{\mathrm{Re}}_{\mathrm{Im}}[\exp(i\omega^a_{\mathrm{iso}}T_R/2) \\ \times f^{aj}{}^*(\gamma)f^{aj}(\gamma + \pi)] \\ \times f^{ai}{}^*(\gamma)f^{ai}(\gamma + \pi + \omega_R t) \\ \times \exp(i\omega^a_{\mathrm{iso}}T_R/2)\exp(i\omega^a_{\mathrm{iso}}t) \quad [13]\end{aligned}$$

instead of Eq. [10]. Taking the echo signal and integrating over the Euler angles finally yields the time-reverse ODESSA spectrum

$$S^-(t;\tau_m) = \sum_a \sum_N (-)^N I^a_N(\tau_m)\exp[i(\omega^a_{\mathrm{iso}} + N\omega_R)t]. \quad [14]$$

This spectrum differs from that of the normal ODESSA sequence, Eq. [11], in two aspects. First, the phase twist has been canceled, and second, for $\tau_m = 0$, it becomes identical to that of the regular MAS spectrum (*16*) without the $(-)^N$ alteration of the spinning side-band phases. [In this limit, the $(-)^N$ of Eq. [14] cancels the $(-)^M$ of Eq. [9].] Such spectra can readily be recorded using the phase cycle indicated by the lower signs in Table 1.

C. Time-Reverse ODESSA in the Presence of Exchange between Different Groups

When the dynamic process involves exchange within the groups of equivalent nuclei as well as between different groups, the latter processes will result in ''phase transfer'' and consequently in phase distortion, even if time-reverse ODESSA is used. In these circumstances, Eq. [13] acquires the form

$$\begin{aligned}{}^{\mathrm{Re}}_{\mathrm{Im}}G(t;\tau_m) \\ = \sum_{bi\,aj} P_{ai\,aj}(\tau_m)\,{}^{\mathrm{Re}}_{\mathrm{Im}}[\exp(i\omega^a_{\mathrm{iso}}T_R/2)f^{aj}{}^*(\gamma)f^{aj}(\gamma + \pi)] \\ \times f^{bi}{}^*(\gamma)f^{bi}(\gamma + \pi + \omega_R t) \\ \times \exp(i\omega^b_{\mathrm{iso}}T_R/2)\exp(i\omega^b_{\mathrm{iso}}t), \quad [15]\end{aligned}$$

and the integration over α, β, γ of the echo signal yields

$$S^-(t;\tau_m) = \sum_b \sum_N (-)^N I^b_N(\tau_m)\exp[i(\omega^b_{\mathrm{iso}} + N\omega_R)t], \quad [16]$$

where

$$\begin{aligned}I^b_N(\tau_m) = \sum_{aj} \sum_i P_{bi\,aj}(\tau_m)\exp[i(\omega^b_{\mathrm{iso}} - \omega^a_{\mathrm{iso}})T_R/2] \\ \times \exp(-\tau_m/T_1^{a,b})I_N^{bi\,aj}. \quad [17]\end{aligned}$$

Here $I_N^{bi\,aj}$ is defined as in Eq. [9]: the summation over the index i refers to the various symmetry-related sites of the b group, the summation over $a\,j$ refers to all the other interchanging sites, and $1/T_1^{a,b}$ is some ill-defined average of $1/T_1^a$ and $1/T_1^b$. When exchange between different groups occurs, phase-twisted components with phase factors, $(\omega^b_{\mathrm{iso}} - \omega^a_{\mathrm{iso}})T_R/2$, appear, for $\tau_m \geqslant k_{ba}^{-1}$, which are different for different families of side bands. These cannot be canceled simultaneously. In fact, even isolated peaks of interchanging nuclei cannot, in general, be phased to pure absorption because they are comprised of components with different phase factors.

EXPERIMENTAL

Cross-polarization (CP) carbon-13 MAS spectra were recorded at 75.47 MHz on a Bruker DSX300 spectrometer. Some measurements were also carried out at 100.6 MHz on a Varian Unity 400 spectrometer. The spinning frequency was kept constant at ± 1 Hz over the entire spinning range used (1–5.3 kHz). The $\pi/2$ pulse widths were 5.0 μs for carbon-13 and 3.1 μs for protons. Cross polarization was effected by a ramp-shaped proton RF pulse with a contact time of 1 ms. The timing of the mixing period was synchronized with the rotor period using optical triggering, as explained in the legend of Fig. 1. In all experiments, *P*1 was a CP pulse, of which the phase was related to that of *P*1 in Table 1 by a $\pi/2$ rotation.

Dimethyl sulfone was obtained commercially. The carbon-13-enriched tropolone samples were prepared as previously described (*8, 13*). 1,4-Diphenoxybenzene was synthesized by reacting 1,4-dibromobenzene and phenol: A mixture of 2.82 g phenol and 1.4 g potassium hydroxide pellets were heated while stirring until dryness. After cooling, 2.36 g of 1,4-dibromobenzene and 50 mg copper–bronze were added, and the mixture was heated to 200°C for three hours, followed by bulb-tube distillation starting at 150°C and 0.1 Torr. The second fraction was allowed to crystallize in the receiver and was then crystallized from ethanol. The yield was 0.9 g of 1,4-diphenoxybenzene; m.p., 72°C; TLC, (CH_2Cl_2/*n*-hexane), one spot.

RESULTS AND DISCUSSION

A. Phase Cycles for Normal and Time-Reverse ODESSA

One of the advantages of the ODESSA experiments lies in the fact that the time-domain signal is obtained by a single phase cycle (Table 1) with no external data manipulation. The correct addition of the cosine and sine components can

be checked by recording spectra at short mixing times. This is demonstrated in Figs. 2 and 3 for the carbon-13 spectra of two model compounds, i.e., isotopically normal dimethyl sulphone (DMS) and tropolone enriched in carbon-13 at the carbonyl and hydroxyl positions to 25 at.% (at each site, but on different molecules).

For a single group of equivalent nuclei, as in DMS, one can always obtain properly phased spectra with the expected MAS intensities (*16*), provided the anti-echo signal is recorded for the normal, and the echo signal for time-reverse ODESSA experiments. The two spectra differ from each other only in the fact that the spinning side bands alternate in the normal and do not alternate in the time-reverse version. This is demonstrated in Fig. 2 for the DMS sample, where both types of ODESSA spectra for short τ_m values are shown. It may be seen that the anti-echo signal of the normal ODESSA (Fig. 2b) and the echo signal of the time-reverse ODESSA (Fig. 2e) yield identical side-band intensities as for the MAS spectrum (Fig. 2a), except that in the former the phases of the spinning side bands alternate. In fact, for a single family of spinning side bands, a linear phase correction can be applied that will interconvert between these two

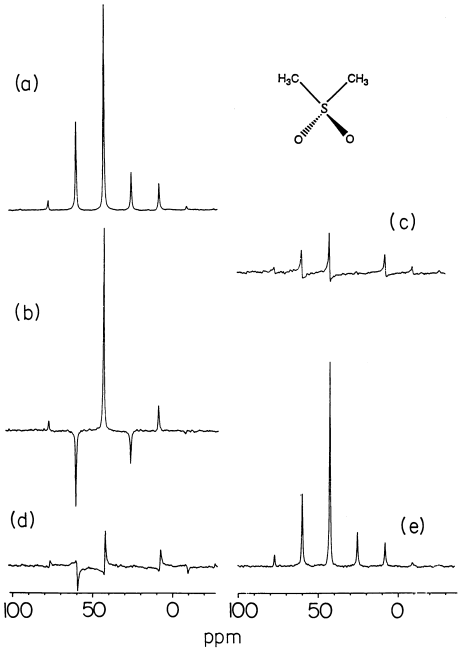

FIG. 2. Room temperature, CP carbon-13 MAS spectra of DMS. All spectra were recorded with ν_R = 1.3 kHz, with 1 ms CP contact time, 1 s recycle time, and a total of 128 scans. (a) Regular MAS spectrum; (b) normal anti-echo and (c) normal echo ODESSA spectra, recorded with a constant phase correction of $\omega_{iso}T_R/2$ relative to that used for the MAS (a); (d) time-reverse anti-echo and (e) time-reverse echo ODESSA spectra, recorded with the same phase setting as in (a). Spectra (b) and (d) were recorded with a mixing time of 3.1 ms (four rotation periods) while for (c) and (e) τ_m was 2.7 ms (3.5 rotation periods). These τ_m values are much shorter than T_1 or k^{-1}. Spectra (b)–(e) were plotted at identical recorder gain, which was twice that used for (a), with LB = 30 Hz.

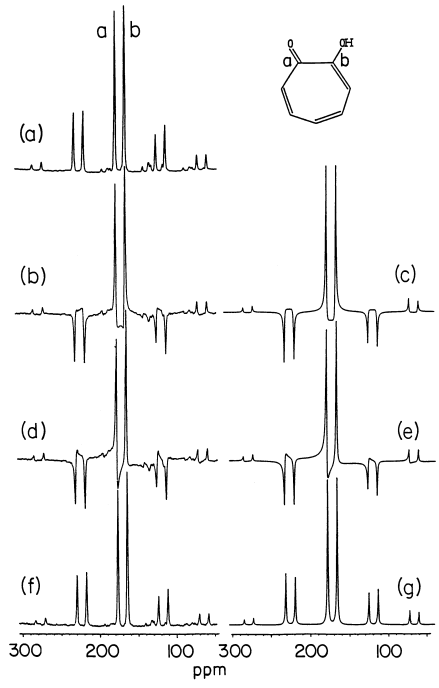

FIG. 3. Room-temperature, CP carbon-13 MAS spectra of tropolone enriched at the carbonyl (a) and hydroxyl (b) sites to 25 at.% ^{13}C (at each site but on different molecules). All spectra were recorded with ν_R = 4.0 kHz with 1 ms CP contact time, 30 s recycle time, and four scans (one full basic phase cycle) per spectrum. (a) Regular MAS spectrum. The weak signals are due to natural-abundance carbon-13 at the other sites of the tropolone molecule. (b) and (c) are experimental and simulated normal anti-echo ODESSA spectra, with the reference frequency halfway between ω^a_{iso} and ω^b_{iso}. (d) and (e) are as (b) and (c), but phase corrected so that the side bands due to the hydroxyl carbon are pure absorption. (f) and (g) are experimental and calculated time-reverse echo ODESSA spectra. The spectra in (b, d, f) were recorded with a mixing time of 100 ms (so that $T_2 < \tau_m \ll T_1, k^{-1}$), at the same gain, which was twice that used for the regular MAS spectrum (a), with LB = 30 Hz. The simulated spectra in (c, e, g) were calculated for $\tau_m = 0$.

modes. If the reverse combination of the Re and Im signals are chosen, i.e., echo for the normal (Fig. 2c) and anti-echo for the time-reverse (Fig. 2d) experiments, both the phases and intensities are in error.

When, however, the spectrum contains more than one type of nucleus as in the enriched tropolone (Fig. 3), the normal ODESSA anti-echo spectrum is phase distorted (Fig. 3b) and when the spinning side bands of one carbon are phased to pure absorption, those of the other carbon become even more distorted (Fig. 3d). On the other hand, the time-reverse ODESSA echo spectrum (Fig. 3f) yields (for short mixing times) properly phased spinning side bands for both types of nuclei. The corresponding simulated spectra on the right-hand side of Fig. 3 were calculated using Eqs. [11] (Figs. 3c and 3e, the latter with constant phase correction) and [14] (Fig. 3g), for $\tau_m = 0$ and the magnetic parameters shown in Table 2. They reproduce well the various effects

TABLE 2

Principal Values of the Chemical-Shift Tensors and Geometrical Parameters Used in the Simulation of the Dimethyl Sulfone and Tropolone Spectra

		Tropolone	
	DMS[a]	a[b]	b[c]
σ_{xx}	19.7	66.0	76.0
σ_{yy}	16.9	32.0	18.0
σ_{zz}	−36.6	−98.0	−94.0
σ_{iso}	43.4	177.8	165.8

[a] For DMS, the *z* axis was taken along the S–CH_3 bond, and the switching angle was taken as 108° about the *y* direction.
[b] Carbonyl carbon.
[c] Hydroxylic carbon.

seen in the experimental spectra, lending support to the proposed procedure.

B. Dynamic Effects in Normal and Time-Reverse ODESSA for a Single Set of Equivalent Nuclei. The Flipping of the DMS Molecule

Equations [11] and [14] show that, for one set of equivalent nuclei undergoing reorientation or spin exchange, the τ_m dependence of the normal and time-reverse ODESSA spectra is the same, differing only in the fact that the phases of the spinning side bands alternate in the normal and do not alternate in the time-reverse versions. Examples of such τ_m-dependent spectra for DMS are shown in Fig. 4. This compound undergoes twofold π flips about the molecular C_2 symmetry axis, resulting in reorientation of the methyl carbon chemical-shift tensor (*11, 12*):

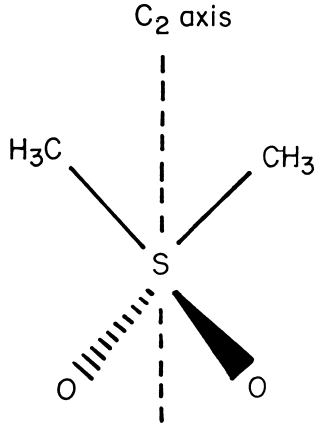

It thus provides an excellent probe molecule for demonstrating dynamic effects involving equivalent nuclei. In this case, there are just two sites, $aj \equiv 1$ and $ai \equiv 2$, and the equations for the side-band intensities (Eq. [8]) become

$$I_N^a(\tau_m) = (\pm)^N \exp(-\tau_m/T_1^a)\{[\tfrac{1}{2}(1 + \exp(-2k\tau_m))]I_N^{11} + [\tfrac{1}{2}(1 - \exp(-2k\tau_m))]I_N^{21}\}, \quad [18]$$

where the +/− signs refer respectively to the normal (Eq. [11]) and time-reverse (Eq. [14]) experiments, and we made use of the fact that $I_N^{22} = I_N^{11}$, $I_N^{12} = I_N^{21}$. Equation [18] can be rearranged to

$$|I_N(\tau_m)| = |(\pm)^N[A_N \exp(-\tau_m/t_1) + B_N \exp(-\tau_m/t_2)]|, \quad [19]$$

where we dropped the superscript *a* and where

$$A_N = \tfrac{1}{2}(I_N^{11} + I_N^{12}); \quad B_N = \tfrac{1}{2}(I_N^{11} - I_N^{12})$$
$$1/t_1 = 1/T_1; \quad 1/t_2 = 1/T_1 + 2k. \quad [20]$$

In Fig. 5 are plotted the absolute normalized intensities, $|I_N(\tau_m)|/|I_0(0)|$, of the center ($N = 0$) and first low field ($N = +1$) side band for the normal and time-reverse experiments of the type shown in Fig. 4, for the entire range of measured mixing times. The results for both experiments are essentially identical and clearly show a bi-exponential decay as expected from Eq. [19]. It may, however, be seen that, although the first decay due to the flipping rate appears

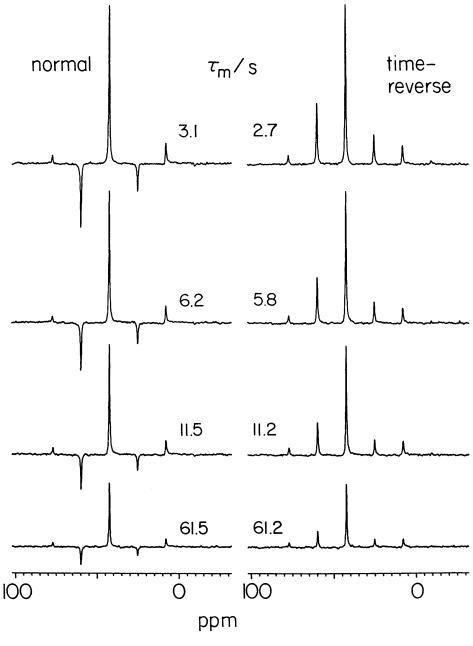

FIG. 4. Examples of normal anti-echo (left) and time-reverse echo (right) ODESSA spectra of DMS with different mixing times. The small difference (0.385 ms) in the mixing times of corresponding spectra in the two columns is due to the fact that they are, respectively, even and odd multiples of half the rotation period. The experimental conditions are the same as described in the legend to Fig. 2. All spectra are plotted with identical recorder gain.

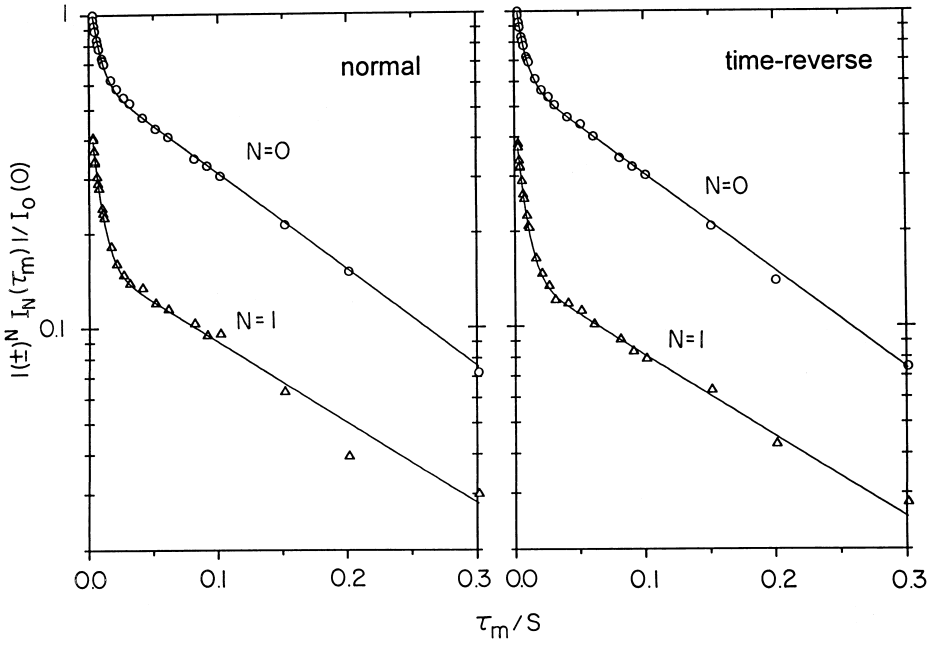

FIG. 5. Semi-logarithmic plots of normalized absolute intensities for the $N = 0$ and $N = +1$ side bands of the normal anti-echo (left) and the time-reverse echo (right) ODESSA spectra of the type shown in Fig. 4, as a function of the mixing time τ_m. The points are experimental. The full lines are calculated from Eq. [17], as explained in the text, with the chemical-shift parameters of Table 2, a switching angle of 108° about the *y* principal direction, T_1 ($N = 0$) = 142 ms, T_1 ($N = +1$) = 171.5 ms, and $k = 72\ s^{-1}$. The measurements were extended up to 500 ms. Only the results for the first 300 ms are displayed.

to be very similar for both lines in both experiments, the second decay, due to T_1, appears to be slightly faster for the center than for the first side band. For a quantitative analysis of the results in Fig. 5, we fixed the coefficients A_N and B_N according to the values of I_N^{ij} calculated from the carbon-13 chemical-shift tensor of the methyl group of DMS (Table 2), assuming a switching angle of 108° about the principal *y* direction, and took the switching rate, k, and the T_1 values of the $N = 0$ and $N = +1$ lines as free parameters. The computed values of I_N^{ij} were $I_0^{11} = 1.596$, $I_0^{12} = 0.0574$, $I_1^{11} = -0.7804$, and $I_1^{12} = 0.3095$, yielding $A_0 = 0.827$, $B_0 = 0.769$, $A_1 = -0.235$, $B_1 = -0.545$, while the best fit results for the kinetic parameters were $k = 71.0\ s^{-1}$, T_1 ($N = 0$) = 142.0 ms, and T_1 ($N = +1$) = 171.5 ms. The full lines through the experimental points in Fig. 5 were calculated using these parameters. As may be seen, the fit is very satisfactory. The result for k is essentially identical to that reported in the previous ODESSA paper (*10*) and in full agreement with a recent deuterium NMR measurement of DMS-d_6 by selective inversion (*12*).

C. Application to the Dynamics of the Ring-Flipping Processes in 1,4-Diphenoxybenzene

We next discuss the ring inversion processes in 1,4-diphenoxybenzene (DPB). The structure and ring-flip dynamics of this compound were studied earlier by X-ray diffraction and carbon-13 MAS NMR spectroscopy by Clayden *et al.* (*14*):

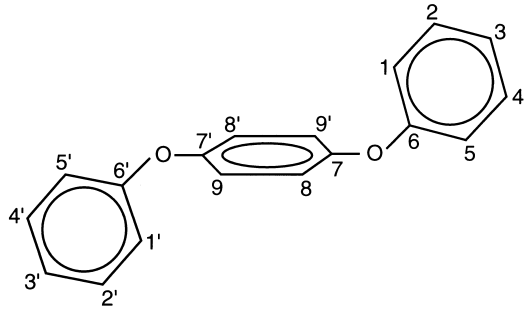

In the crystalline state, the DPB molecule is centro-symmetric, with the terminal phenoxy rings in a trans coplanar arrangement and the center benzene in a nearly orthogonal plane. The carbon-13 MAS spectrum, at room temperature, consists of eight resolved peaks and is essentially identical to that of the time-reverse ODESSA spectrum for short τ_m, shown in the upper traces of Fig. 6. The peak assignments, as determined by Clayden *et al.* (*14*), are also given in the figure. On heating to above room temperature, π flips of the outer phenoxy rings result in gradual broadening and pairwise coalescence of the (1, 5) and (2, 4) doublets, while the signal of the degenerate

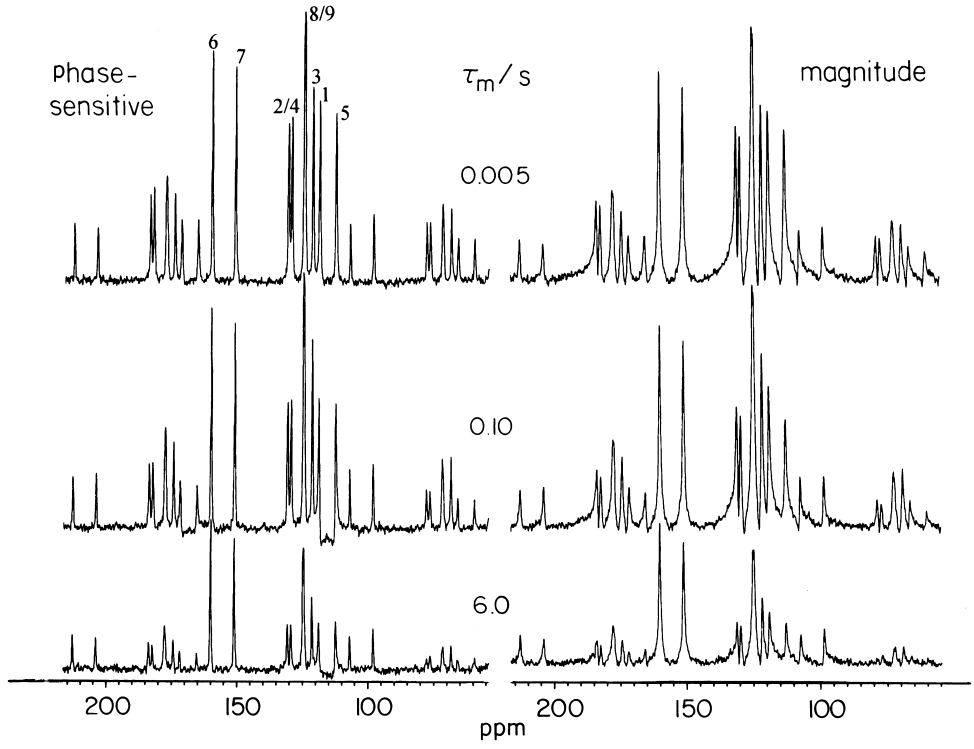

FIG. 6. Carbon-13 time-reverse echo ODESSA spectra (at 75.47 MHz) of DPB recorded at 21°C with the indicated mixing times. The rotation frequency was 4.0 kHz; recycle time, 20 s; 480 scans; CP contact time, 1 ms; and LB = 15 Hz. Only the center band and the $N = \pm 1$ spinning side bands are displayed. (Left) Phase-sensitive spectra with the same phase setting as used to obtain a pure-absorption MAS spectrum. (Right) Magnitude spectra. The assignments of the center band peaks are given on the upper trace in the left column.

carbons, 8 and 9, due to the inner benzene ring remains sharp. Neither is any broadening observed for the resonances of the para carbons 3, 6, and 7 (*14*). The chemical-shift tensors of the para carbons are not modulated by π flips of the benzene rings, and therefore no broadening is expected. On the other hand, the lack of broadening of the peak due to the ortho/meta carbons (*8, 9*) does not, necessarily, rule out flipping of the inner benzene ring, since such an effect would be minimized by the fast-spinning rate employed in Clayden's experiments. Moreover, if such a flip process were in the slow-exchange regime, it would have no effect on the MAS spectrum even at much slower spinning rates. The time-reverse ODESSA experiment is ideally suited to determine whether such a slow flipping process occurs and, if it does, to determine its rate.

Examples of carbon-13 time-reverse ODESSA spectra are shown in the left column of Fig. 6 for several mixing times. These spectra were recorded at 21°C with a spinning rate of 4 kHz. Only the center band and the $N = \pm 1$ spinning side bands are displayed. The spectrum at $\tau_m = 5$ ms is essentially the same as that from MAS. With increasing mixing time, there is a gradual, but differential, decay of all peaks. The most rapidly decaying ones are those associated with carbons 2, 4, 1, and 5, with the latter two also undergoing phase twists. The intensities of all the center peaks ($N = 0$) are plotted as a function of τ_m in Fig. 7. The intensities of the twisted peaks, 1 and 5, were somewhat arbitrarily taken as the span between their maximum and minimum points. The results so obtained are indicated by the solid symbols in Fig. 7. They are divided into three diagrams: the left one corresponds to the ortho/meta carbons (2, 4, 1, 5) of the phenoxy rings, the middle one to the ortho/meta (8, 9) carbons of the center benzene ring, and the right one to the para carbons in the molecule (6, 7, 3). The open symbols for the 8/9 carbons are for higher temperatures, as indicated, and will be discussed shortly. As indicated above, the para carbons are not affected by ring flips. They exhibit simple exponential decay, which must be associated with their T_1 relaxation. The T_1 values derived from these decay curves are given in Table 3.

The more interesting results are those for the peak associated with carbons 8/9 of the center benzene ring. The decay of this signal, as shown by the solid squares in the center column in Fig. 7, is clearly not monoexponential and suggests the occurrence of exchange within this group of equivalent nuclei on the time scale of 1 s. We identify this exchange with the π flipping of the center benzene ring of the DPB molecule. To substantiate this interpretation, we repeated the time-reverse ODESSA experiments on this compound at higher temperatures. We expect that, with increasing temperature, the flipping rate of the center ring will increase and

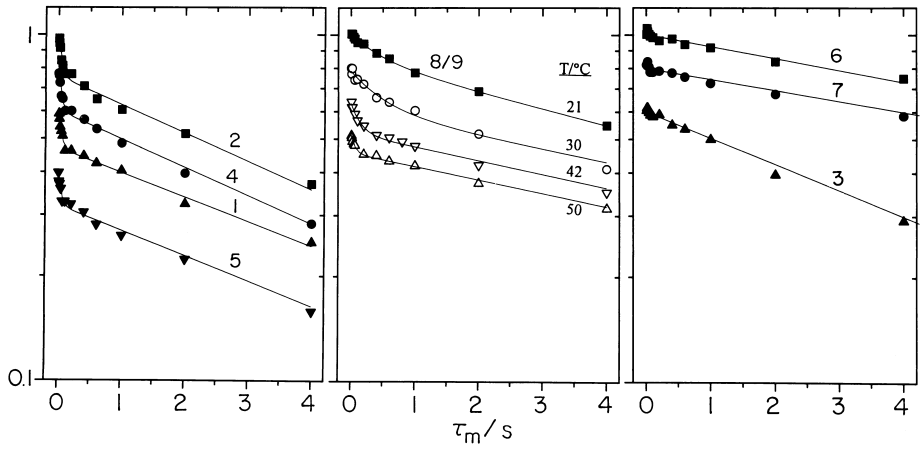

FIG. 7. Semi-logarithmic plots of the peak intensities in the time-reverse ODESSA experiments of DPB as a function of the mixing time. The data in solid symbols were obtained at 21°C under the same experimental conditions as those described in the legend to Fig. 6. The open symbols correspond to data recorded at 100.6 MHz with a spinning rate of 5.33 kHz at the indicated temperatures. To separate the various decay curves in each diagram, the initial points were normalized to different values (1.0 for carbon 2, 0.8 for 4, 0.6 for 1, and 0.4 for 5 in the left diagram; 1, 0.8, 0.64, and 0.51 for 21°C, 30°C, 42°C and 50°C, respectively, in the center diagram for carbons 8/9; and 1.0 for carbon 6, 0.8 for 7, and 0.6 for 3 in the right diagram). Measurements were extended up to 20 s. Only the results for the first 4 s are displayed in the diagrams. The full lines were calculated using Eq. [19], as explained in the text, with the rate parameters of Table 3 for 21°C and those given in the text for the higher temperatures.

render the biexponentiality of the 8/9 decay curve more pronounced. These higher-temperature measurements were carried out at 100.6 MHz with a spinning rate of 5.33 kHz so as to keep the same ratio of ω_R/ω_0 as for the 21°C experiments. The signals due to the 8/9 and all the para carbons remain sharp upon heating, while those for the ortho and meta carbons of the phenoxy rings undergo pairwise coalescence due to π flipping of the outer rings, as described by Clayden *et al.* (*14*). The decay of the 8/9 signal as a function of the mixing time is indicated by open symbols in the center column of Fig. 7. As anticipated, with increasing temperature the initial decay, due predominantly to the flipping process of the center benzene ring, becomes steeper. For a quantitative analysis of these results, we used Eq. [19], with the superscript 8 and 9′ (or 8′ and 9) instead of 1 and 2. However, rather than calculating A_0 and B_0 from the anisotropic chemical-shift tensors of these carbons (*14*), we took the ratio B_0/A_0 as a free parameter and fitted the flip rate, k^B, and $T_1^{8,9}$ to the experimental decay curve. The results for 21°C are included in Table 3. The k^B values at higher temperatures were 0.9 s^{-1} at 30°C, 3.2 s^{-1} at 42°C, and 7.5 s^{-1} at 50°C, with essentially the same T_1 (11 s) over the temperature range of the measurements. The results for k around room temperature are less accurate, because the two decay rates (k^B and $1/T_1^{8,9}$) are not much different. Taking an average value of k^B at 25°C of 1 s^{-1} together with the results at higher temperatures yields an estimated activation energy of 16 kcal mol^{-1} for the flip process. The fitted B_0/A_0 ratio varied between 0.13 and 0.29 with an average of 0.20, while a ratio of $B_0/A_0 = 0.11$ was calculated from the chemical-shift tensors estimated by Clayden *et al.* (*14*). Considering the uncertainties involved in estimating the carbon chemical-shift tensors and the difficulties in analyzing biexponential decays, the agreement is quite reasonable.

TABLE 3

Magnetic and Rate Parameters for 1,4-Diphenoxybenzene as Determined from the Time-Reverse ODESSA Experiments at 21°C

	Carbon							
	2	4	1	5	8/9	6	7	3
σ_{iso} (ppm)	131.0	129.7	119.05	112.8	124.96	160.5	151.6	121.66
B_0/A_0	0.33	0.34	0.29	0.26	0.18	—	—	—
k (s^{-1})	11.1	11.6	11.4	11.1	0.96	—	—	—
T_1 (s)[a]	5.3	5.3	6.1	6.0	9.0	15.3	13.8	5.8
T_1^{IR} (s)[b]	9.3	9.3	10.5	10.5	15.8	25.0	26.6	9.5

[a] Results obtained from the analysis of the time-reverse ODESSA experiments.
[b] Results obtained from independent inversion-recovery experiments.

The flip rate of the center benzene ring is more than an order of magnitude slower than that of the outer phenoxy rings and is consistent with the explanation given by Clayden (*14*) for the lack of broadening of the 8/9 peak on heating the DPB to above 60°C. This also confirms the conclusion (*14*) that flipping of the various rings in DPB is not a concerted process.

As may be seen in the left diagram of Fig. 7, the peaks due to the ortho/meta carbons of the phenoxy rings exhibit very pronounced biexponential decays reflecting their much faster flip rate. Since the interchanging carbons 1, 5 and 2, 4 are not equivalent, the more appropriate method to study their interconversion in the slow-exchange regime would be by one of the MAS polarization-transfer techniques (*1–3*). Nevertheless, for completeness and to show the difficulties with ODESSA spectroscopy for exchange between inequivalent nuclei, we briefly discuss these spectra and present a qualitative analysis. The relevant expression for two nonequivalent interchanging sites can be obtained from Eq. [17], by considering just two groups of nuclei, a and b,

$$I_N^a(\tau_m) = \left\{\frac{1}{2}[1 + \exp(-2k^P\tau_m)]I_N^{aa} + \frac{1}{2}[1 - \exp(-2k^P\tau_m)] \times \exp[i(\omega_{iso}^a - \omega_{iso}^b)T_R/2]I_N^{ab}\right\}\exp(-\tau_m/T_1)$$

$$= \frac{1}{2}[\{I_N^{aa} + I_N^{ab}\exp[i(\omega_{iso}^a - \omega_{iso}^b)T_R/2]\}\exp(-\tau_m/T_1) + \{I_N^{aa} - I_N^{ab}\exp[i(\omega_{iso}^a - \omega_{iso}^b)T_R/2]\}$$

$$\times \exp[-(2k^P + 1/T_1)\tau_m]]$$

$$= A_N\exp(-\tau_m/t_1) + B_N\exp(-\tau_m/t_2), \qquad [21]$$

where k^P is the flip rate of the phenoxy rings, A_N, B_N, T_1, and t_2 are defined in a similar way as in Eq. [20], except that now A_N and B_N are complex, and a, b refer to the pairs of carbons 1, 5 or 2, 4. We also dropped the indices i, j since there is only one site in each group. For $\tau_m \geqslant (k^P)^{-1}$, these signals thus comprise two components with different phases. They can, therefore, not be phased to pure absorption. At a phase setting which gives absorption MAS spectra, these pairs gradually develop a component with a phase twists of $\pm(\omega_{iso}^a - \omega_{iso}^b)T_R/2$, which is manifested by the trough between the peaks due to carbons 1 and 5 in Fig. 6. The chemical-shift difference between carbons 2 and 4 is apparently too small to develop a clear trough, but a twist in that direction is clearly observed in the spectra of Fig. 6.

For a quantitative analysis of these changes in terms of the phenoxy ring flips, it is necessary to compare the experimental lineshapes with simulations of Eq. [21]. Instead of such a full analysis, we preferred a more qualitative approach and approximated the peak intensities of carbons 1 and 5 as the span between the maxima and minima of their phase-twisted signals, while for carbons 2 and 4 the full peak heights were taken. These approximate intensities are plotted in the left diagram of Fig. 7. We then analyzed these results in terms of Eq. [21], taking the various A_0/B_0 values as real free parameters and fitting the curves in terms of k^P and T_1. The results are included in Table 3. The average result for k^P is 11.3 s^{-1}, about one-half that estimated from the kinetic parameters given by Clayden *et al.* (*14*) for this reaction. Clearly, because of the approximations employed, our results give only a rough estimate for k^P. A quantitative analysis could, of course, be made by a full lineshape analysis, but the classical MAS-polarization transfer experiments (*2, 3*) would be more suitable for such measurements. Alternatively, magnitude spectroscopy could be used. However, although the expressions for the line intensities can be derived in a straightforward way, they are cumbersome, and the spectra are badly twisted, as can be seen in the right-hand column of Fig. 6.

D. Time-Reverse ODESSA Spectra of Enriched Tropolone

Tropolone in the solid state was shown by carbon-13 MAS 2D exchange NMR (*2*) to undergo tautomeric hydrogen shift of the form

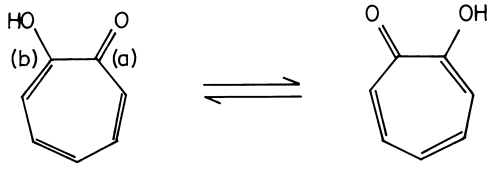

It was subsequently found (*6*) that this process reflects self-diffusion in the crystal between different symmetry-related crystallographic sites, the hydrogen shift being only a secondary process that occurs whenever the molecule finds itself in a flipped orientation in the lattice. There are four tropolone molecules in the unit cell arranged in two centrosymmetric hydrogen-bonded dimers (*17*). For interpretation of NMR data, we need, therefore, consider only two symmetry-related, but in general magnetically inequivalent, molecules in the crystal. If we consider only the labeled carbons in the enriched tropolone sample, already discussed in part A of this section, the following sites

may be distinguished: a1, a2, b1, and b2, where the first index refers to the carbonyl (a) and hydroxyl (b) carbons in each molecule and the second index, 1 and 2, to the two magnetically distinguishable molecules in the unit cell. There are thus three types of exchange processes that must be considered:

1. Molecular flips (or flip-jumps to identical crystallographic sites) accompanied by proton transfer. This leads to interchanges of the type a1 ⇄ b1 and a2 ⇄ b2.
2. Molecular jumps to a symmetry-related site without hydrogen shift: a1 ⇄ a2; b1 ⇄ b2.
3. Molecular jumps to a symmetry-related site with proton transfer: a1 ⇄ b2; b1 ⇄ a2.

We label the rate constants for these processes k_1, k_2, and k_3 respectively, so that the exchange matrix becomes

$$\mathbf{K} = \begin{array}{c|cccc} & a1 & b1 & a2 & b2 \\ \hline a1 & -k & k_1 & k_2 & k_3 \\ b1 & k_1 & -k & k_3 & k_2 \\ a2 & k_2 & k_3 & -k & k_1 \\ b2 & k_3 & k_2 & k_1 & -k \end{array} \qquad [22]$$

where $k = k_1 + k_2 + k_3$. Of these exchange mechanisms, only the second, characterized by the rate constant k_2, corresponds to pure reorientation, while k_1 and k_3 involve exchange between different groups of spins. In the time-reverse ODESSA experiment, k_2 will only affect the peak intensities, but k_1 and k_3 will also lead to phase distortion. To apply the equations derived above for the ODESSA experiments, we need to solve Eq. [2] for the $P_{ij}(\tau_m)$ values. Recalling that all the magnetizations have identical equilibrium populations, $P_{a1} = P_{b1} = P_{a2} = P_{b2} = 1$, we obtain

$$\begin{aligned} \mathbf{P}(\tau_m) &= \exp(\mathbf{K}\tau_m) \\ &= \mathbf{S}^{-1}\exp(\mathbf{\Lambda}\tau_m)\mathbf{S} \\ &= \begin{bmatrix} a & b & c & d \\ b & a & d & c \\ c & d & a & b \\ d & c & b & a \end{bmatrix}, \end{aligned} \qquad [23]$$

where $\mathbf{P}(\tau_m)$ is the matrix of the $P_{ij}(\tau_m)$ values, $\mathbf{\Lambda}$ is the diagonal matrix of the eigenvalues of $\mathbf{K}$, and $\mathbf{S}$ is the matrix of its eigenvectors, so that $\mathbf{SKS}^{-1} = \mathbf{\Lambda}$, with

$$\mathbf{S} = \tfrac{1}{2}\begin{bmatrix} 1 & 1 & 1 & 1 \\ 1 & -1 & -1 & 1 \\ -1 & 1 & -1 & 1 \\ -1 & -1 & 1 & 1 \end{bmatrix}$$

$$\mathbf{\Lambda} = \begin{bmatrix} 0 & & & \\ & -2(k_1 + k_2) & & \\ & & -2(k_1 + k_3) & \\ & & & -2(k_2 + k_3) \end{bmatrix} \qquad [24]$$

and

$$\begin{aligned} a &= 1 + \exp[-2(k_1 + k_2)\tau_m] \\ &\quad + \exp[-2(k_1 + k_3)\tau_m] \\ &\quad + \exp[-2(k_2 + k_3)\tau_m] \\ b &= 1 - \exp[-2(k_1 + k_2)\tau_m] \\ &\quad - \exp[-2(k_1 + k_3)\tau_m] \\ &\quad + \exp[-2(k_2 + k_3)\tau_m] \\ c &= 1 - \exp[-2(k_1 + k_2)\tau_m] \\ &\quad + \exp[-2(k_1 + k_3)\tau_m] \\ &\quad - \exp[-2(k_2 + k_3)\tau_m] \\ d &= 1 + \exp[-2(k_1 + k_2)\tau_m] \\ &\quad - \exp[-2(k_1 + k_3)\tau_m] \\ &\quad - \exp[-2(k_2 + k_3)\tau_m]. \end{aligned} \qquad [25]$$

In the enriched tropolone sample, spin diffusion will also cause spin exchange between the various carbons and thus mask the effect of chemical exchange (*8, 13*). To eliminate the latter effect, we decided to include proton decoupling in the pulse sequence during the mixing time (*18*). In order to determine the decoupling level required for complete quenching of spin diffusion, we performed magnetization-transfer experiments between the carbonyl and hydroxyl carbons, by inverting one of the two signals in a preparation period and monitoring the approach to equilibrium as a function of τ_m for different decoupling power (*2, 8*). The results of these experiments on the 25 at.%-enriched tropolone sample, expressed as $[I_0^b(\tau_m) - I_0^a(\tau_m)]/[I_0^b(0) - I_0^a(0)]$ versus τ_m, are plotted in the left diagram of Fig. 8. Here I_0^a and I_0^b refer to the intensities of the center band of carbonyl (a) and hydroxyl (b). It may be seen that, with increasing decoupling power, there is a significant reduction in the rate of magnetization transfer. However, no asymptotic value of the decay rate was reached even at the highest power level used, indicating that spin diffusion was not completely quenched. We therefore repeated the magnetization-transfer experiment on a less-enriched sample which contained only 5 at.% carbons-13 at each of the sites *a* and *b*. The results so obtained are plotted in the right diagram of Fig. 8. It may be seen that now an asymptotic decay rate is reached, well below the maximum decoupling power. In fact, the asymptotic rate corresponds closely to that measured in isotopically normal tropolone (*2*), in which spin diffusion can be completely neglected on the time scale of the experiment. The time-reverse ODESSA experiments were therefore performed on the 5% sample with proton decoupling using the two-pulse phase-modulation (TPPM) sequence (*19*) during the mixing time at a level corresponding to −6dB (∼10 W).

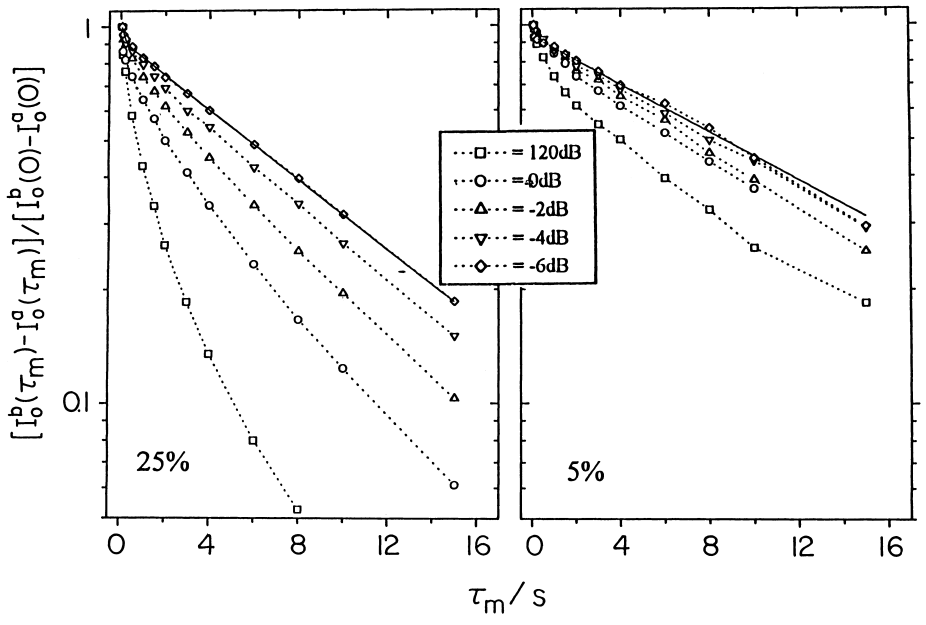

FIG. 8. Carbon-13 MAS magnetization-transfer experiments between the carbonyl (a) and hydroxyl (b) carbons in 25 and 5 at.%-enriched tropolone at room temperature, using different proton decoupling levels as indicated. The rotation frequency was 4 kHz. The highest decoupling power (−6 dB) corresponds to approximately 10 W. The solid lines in the two diagrams correspond to decay rates of 0.054 s^{-1} (left) and 0.036 s^{-1} (right).

Examples of time-reverse ODESSA spectra for the 5 at.%-enriched sample at different mixing times, with proton decoupling are shown in Fig. 9. The overall peak intensities, $I_0^a(\tau_m)$, measured as above for DPB and normalized with respect to $I_0^a(0)$, are plotted in Fig. 10 as a function of the mixing time on a linear-log scale. Also plotted is the ''effective phase difference,'' $\delta\phi$, between the (a) and (b) signals. This was obtained in the following way: When phase-distorted spectra started to appear (at $\tau_m \gtrsim 1$ s), a phase correction was applied so as to make one family of side bands (say that of a) appear in pure absorption. A constant phase correction was then applied until the second family of side bands appeared in pure absorption. The change in the constant phase setting so obtained is defined as $\delta\phi$ in the upper part of Fig. 10. This effective phase difference is only a qualitative measure of the extent of exchange between different groups. As indicated above, such exchange-distorted signals cannot, in principle, be phased.

It may be seen that up to $\tau_m \sim 1$ s there is some decrease in the peak intensity, followed by a steeper decrease which is accompanied with a significant phase twist. Recalling that T_1 of tropolone is about 40 s at room temperature (*2*), the two initial dispersion regions may be associated with k_2, which corresponds to pure reorientation, and k_1 plus k_3, which also involve interchange of peaks (a) and (b). A quantitative analysis of these results is, however, quite difficult. First, the effect on the intensity for $\tau_m \lesssim 1$ s is small, while at around 10 s the effect of T_1 cannot be ignored. The small effect of k_2 on the peak intensities is due to the fact that the chemical-shift tensors in the two sites are quite

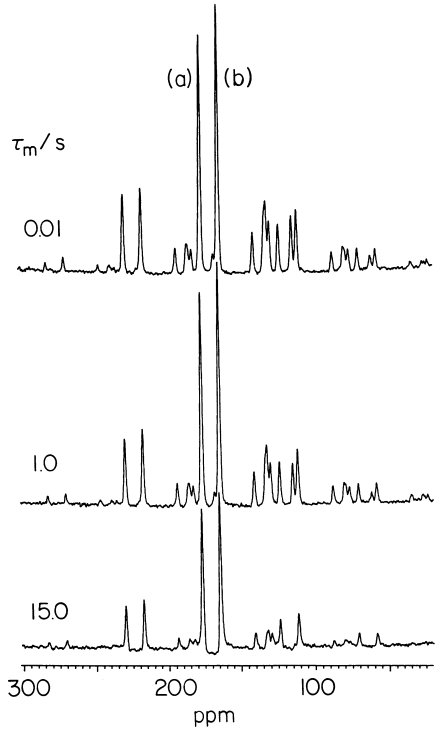

FIG. 9. Carbon-13 time-reverse echo ODESSA spectra of the tropolone sample enriched to 5 at.% at positions (a) and (b), using different mixing times as indicated. Experimental conditions are as described in the legend to Fig. 3. Peaks due to natural-abundance carbon-13 in the other sites of the tropolone molecule are also observed.

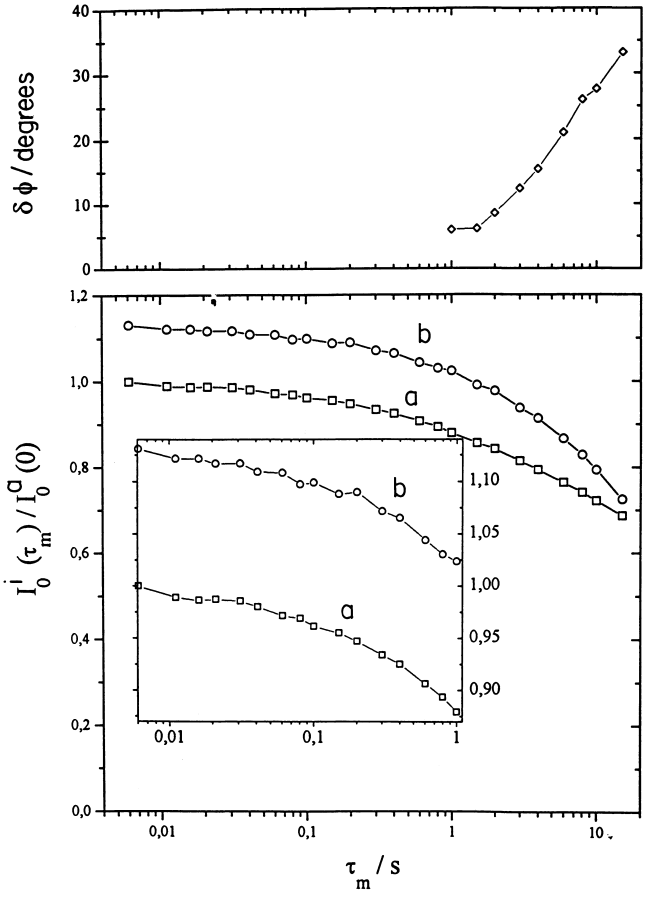

FIG. 10. (Bottom) Plots of the normalized intensities of the carbonyl (a) and hydroxyl (b) peaks in the time-reverse ODESSA experiment described in the legend to Fig. 9 as a function of the mixing time, τ_m. (Top) The effective ''phase factor difference'' between the signals of carbons (a) and (b) as a function of the mixing time. For both diagrams, the scale of the ordinate is linear, while that for τ_m is logarithmic.

similar and the effective reorientation angle is not large (*13*). The $I_{MN}^{bj\,aj}$ for $M \neq N$ are therefore very small compared to those with $M = N$, and the ODESSA experiment becomes insensitive to the exchange process. It appears that, in the case of tropolone, the ODESSA experiment is not suitable for a kinetic analysis, and the full 2D exchange experiment (*6*) must be used.

SUMMARY AND CONCLUSIONS

We have extended the ODESSA 1D exchange experiment for magic-angle-spinning samples, which was originally designed for a single group of equivalent nuclei (*10*), to systems with several such groups undergoing internal exchange. The new method, which we call time reverse ODESSA, makes use of ideas introduced earlier to obtain pure-absorption spectra in rotor-synchronized 2D exchange experiments (*5*). The extension is important because it provides a simple 1D method for using carbon-13 NMR to study reorientation in systems such as polymers, glasses, and molecular crystals, which usually exhibit a multitude of signals. The experiment is easy to perform, and the spectra can be accumulated using a single set of phase-cycled sequences, without extra data manipulation. For many purposes, it provides a substitute for the much more time-consuming 2D exchange procedures.

The experiment is, however, not a general method. If mutual exchange between different groups of equivalent nuclei takes place in addition to pure reorientation, the spectrum will be phase twisted and difficult to analyze, although it could be used to discriminate between pure reorientation and chemical exchange. Also, under certain conditions, the experiment is insensitive to the dynamic process. This can, however, be checked by simulation if the anisotropic tensors are known, and one can then always resort to the 2D exchange experiment, where the correlation terms are directly detected as cross peaks.

Finally, we wish to indicate a difficulty that was also mentioned in the original publication of the ODESSA experiment (*10*). When T_1 values derived from ODESSA are compared with those obtained directly from inversion recovery experiments, the latter values are often significantly longer than the former values. As an example, we include in Table 3, T_1 values for DPB obtained by inversion recovery, where the effect is well demonstrated. A related difficulty was already mentioned in connection with the DMS results, where the best-fit T_1 values for different spinning side bands were quite different and shorter than the value obtained by inversion recovery. The ODESSA results for T_1 of the $N = 0$ and $N = +1$ spinning side bands are 142 and 171.5 ms, respectively, while from inversion recovery, the value is 194 ms for both. We have no explanation for these discrepancies.

ACKNOWLEDGMENTS

We thank Professor Shimon Vega for helpful discussions. This research was supported by a grant from the United States–Israel Binational Science Foundation (BSF), Jerusalem, Israel.

REFERENCES

1. N. M. Szeverenyi, M. J. Sullivan, and G. E. Maciel, *J. Magn. Reson.* **47,** 462 (1982).
2. N. M. Szeverenyi, A. Bax, and G. E. Maciel, *J. Am. Chem. Soc.* **105,** 2579 (1983).
3. C. Connor, A. Naito, K. Takegoshi, and C. A. McDowell, *Chem. Phys. Lett.* **113,** 123 (1984).
4. A. F. DeJong, A. P. M. Kentgens, and W. S. Veeman, *Chem. Phys. Lett.* **109,** 337 (1984).
5. A. Hagemeyer, K. Schmidt-Rohr, and H. W. Spiess, *Adv. Magn. Reson.* **13,** 85 (1989).
6. J. J. Titman, Z. Luz, and H. W. Spiess, *J. Am. Chem. Soc.* **114,** 3756 (1992).
7. Z. Luz, H. W. Spiess, and J. J. Titman, *Isr. J. Chem.* **32,** 145 (1992).
8. Z. Olender, D. Reichert, A. Müller, H. Zimmermann, R. Poupko, and Z. Luz, *J. Magn. Reson. A* **120,** 31 (1996).

9. Y. Yang, M. Schuster, B. Blümich, and H. W. Spiess, *Chem. Phys. Lett.* **139,** 239 (1987).
10. V. Gérardy-Montouillout, C. Malveau, P. Tekely, Z. Olender, and Z. Luz, *J. Magn. Reson. A* **123,** 7 (1996).
11. M. S. Solum, K. W. Zilm, J. Michl, and D. M. Grant, *J. Phys. Chem.* **87,** 2940 (1983).
12. M. J. Brown, R. L. Vold, and G. L. Hoatson, *Solid State NMR* **6,** 167 (1996).
13. R. G. Larsen, Y. K. Lee, B. He, J. O. Yang, Z. Luz, H. Zimmermann, and A. Pines, *J. Chem. Phys.* **103,** 9844 (1995).
14. N. J. Clayden, D. Williams, and C. A. O'Mahoney, *J. Chem. Soc. Perkins Trans.* **2,** 729 (1990).
15. D. Reichert, Z. Olender, R. Poupko, H. Zimmermann, and Z. Luz, *J. Chem. Phys.* **98,** 7699 (1993).
16. J. Herzfeld and A. E. Berger, *J. Chem. Phys.* **73,** 6021 (1980).
17. H. Shimanouchi and Y. Sassada, *Acta Crystallogr. Sect. B* **29,** 81 (1973).
18. H.-H. Limbach, B. Wehrle, M. Schlabach, R. Kendrick, and C. S. Yannoni, *J. Magn. Reson.* **77,** 84 (1988).
19. A. E. Bennet, C. M. Rienstra, M. Auger, K. V. Lakshmi, and R. G. Griffin, *J. Chem. Phys.* **103,** 6951 (1995).